Pilot-Aided OFDM Channel Estimation in the Presence of the Guard Band

Seongwook Song and Andrew C. Singer

***Abstract*—In this letter, pilot design and channel estimation are discussed for orthogonal frequency-division multiplexing (OFDM) systems with guard subcarriers. First, we investigate the effects of guard band on channel estimation errors. From this, we propose pilot placement having a maximum distance between adjacent pilots except for the guard band, and show that it achieves minimum channel estimation errors among partially equispaced pilots using equivalence of the Toeplitz and circulant matrices. Also, an efficient channel estimator is developed by introducing an extended channel and its finite impulse response (FIR) approximation to overcome high numerical complexity caused by the presence of guard subcarriers and the use of a large number of subcarriers. Simulation results are presented for OFDM and orthogonal frequency division multiple access (OFDMA) systems consistent with IEEE 802.16a standards.**

***Index Terms*—Channel estimation, orthogonal frequency-division multiplexing (OFDM), orthogonal frequency division multiple access (OFDMA), pilot design.**

I. Introduction

ORTHOGONAL frequency division multiplexing (OFDM) supports a high data rate in time delay spread environments with efficient equalization. As equalization requires channel state information (CSI), pilots on predetermined subcarriers are sent as training signals in OFDM systems, and the channels for pilot subcarriers are directly estimated, while those for nonpilot subcarriers need to be estimated through interpolation with the channel estimates from adjacent pilot subcarriers. The optimal pilots to minimize the mean-squared error (MSE) or to maximize channel capacity for single antenna OFDM systems are discussed in [4]–[6], and those for more general cases such as multiple antenna systems recently in [7]. In summary, minimum mean-squared error (MMSE) optimal pilots should be equal-power and equidistance for single antenna OFDM systems, referred to as *comb pilots*, while the additional condition of phase-shift orthogonality should be imposed for multiple antenna systems for complete separation of channels associated with different transmitting antennas in the time domain. Instead of sending the comb pilots each OFDM symbol, one OFDM symbol can be dedicated only for training purpose, referred to as *block pilots* in this paper.

As for channel estimation, there have been a variety of algorithms with different optimization criteria and levels of numerical complexity. For example, linear interpolation is a simple and practical method but exhibits a performance floor [8]. In [9], a frequency domain MMSE estimator was proposed, and time domain maximum likelihood (ML) and MMSE estimators were also studied under the condition that channels in OFDM systems are finite impulse response (FIR) of length significantly smaller than the total number of subcarriers [10]. In case that the time-frequency domain channel statistics such as delay spread and Doppler frequency are known to the receiver, the MMSE criterion leads to the 2-D interpolator, which can be implemented by 2-D fast Fourier transform (FFT) and inverse fast Fourier transform (IFFT) in [11], [12].

However, previous work in many literature studied the optimal pilot design and the associated channel estimator under rather unrealistic assumption that all subcarriers in OFDM systems are usable, while in practice, a considerable portion of subcarriers are reserved as guard subcarriers to avoid possible interference from neighboring communication channels. In this paper, we discuss the least squares (LS), ML, and MMSE channel estimators in the presence of guard subcarriers and their performance in terms of the MSE. Since guard subcarriers limit the use of comb pilots in many standards such as [2], we take into account more general pilots, such as the partially equispaced pilots, which have an equal distance between all possible pairs of neighboring pilots except for those crossing guard bands. With the aid of certain asymptotic equivalence properties of Toeplitz and circulant matrices, we investigate the eigenstructure of the product of the associated discrete Fourier transform (DFT) matrix, which frequently appears in expressions of the MSE, and show that among partially equispaced pilots, the one with maximum distance from adjacent pilots achieves the minimum channel estimation error. In addition, to reduce numerical complexity incurred from the presence of guard subcarriers, we develop a suboptimal channel estimator based on an extended channel and its FIR approximation, and discuss its implementation with a low-pass filter (LPF).

The rest of this paper is organized as follows. Section II reviews a system model and channel estimation in the presence of guard subcarriers. The effects of guard subcarriers on channel estimators and pilot design are discussed in Section III. Sections IV discuss a suboptimal channel estimator and its implementations. Finally, conclusions are made in Section V.

II. Pilot-Aided Channel Estimation

In a conventional OFDM system, a stream of data $s(k) \in \mathcal{A}$ is concatenated into a length N signal vector, $\boldsymbol{s} := (s(0), s(1), \ldots, s(N-1))^T \in \mathcal{A}^N$, through serial to parallel conversion, where $()^T$ denotes the transposition operator and $\mathcal{A}$ denotes M-ary alphabet. Signal vectors $\boldsymbol{s}$ are modulated with the inverse DFT (IDFT). After insertion of a cyclic prefix of length N_c, serially converted data is transmitted through

Paper approved by Y. Li, the Editor for Wireless Communication for the IEEE Communications Society. Manuscript received September 24, 2004; revised July 17, 2005 and August 4, 2005.

S. Song is with Samsung Electronics Company, Ltd. Gyeonggi 442-600, Korea (e-mail: seongwook.song@samsung.com).

A. C. Singer is with Coordinated Science Laboratory, University of iIlinois at Urbana-Champaign, Urbana, IL 61801 USA (e-mail: acsinger@uiuc.edu).

Digital Object Identifier 10.1109/TCOMM.2007.902526

a length L time-invariant FIR channel $h[n]$. At the receiver, the received signal $x[n]$ is converted, through serial to parallel conversions, to a vector $\boldsymbol{x} \in \mathcal{C}^{N+N_c}$. The interference from neighboring OFDM symbols can be eliminated by removing the cyclic prefix from $\boldsymbol{x}$. Finally, the output from the cyclic prefix removal $\boldsymbol{x}_c \in \mathcal{A}^N$ is processed with the N-point DFT to result in $\boldsymbol{y} := (y(0), y(1), \ldots, y(N-1))^T$, which can be written as

$$\boldsymbol{y} = \boldsymbol{F}_{N,N}\boldsymbol{x}_c = \text{diag}((\check{h}(0), \check{h}(1), \ldots, \check{h}(N-1))^T)\boldsymbol{s} + \boldsymbol{w} \tag{1}$$

where $\check{h}(k)$ is the N-point DFT of $(h[0], h[1], \ldots, h[L-1], 0, \ldots, 0)^T$, $\text{diag}(\boldsymbol{\theta})$ denotes a diagonal matrix with $\boldsymbol{\theta}$ as its diagonal entries, and

$$[\boldsymbol{F}_{N,K}]_{l,k} = e^{-j\frac{2\pi}{N}(l-1)(k-1)}, \qquad 1 \leq l \leq N, 1 \leq k \leq K$$

and $[\boldsymbol{A}]_{i,j}$ denotes ith row and jth column entry of the matrix $\boldsymbol{A}$, and $\boldsymbol{w} := (w(0), w(1), \ldots, w(N-1))^T$ with $\text{cov}[\boldsymbol{w}] = N_0\boldsymbol{I}_N$. Consequently, OFDM reshapes the frequency selective channel into N single tap non intersympoi interference (ISI) channels, and given $\check{h}(k)$, the transmitted symbol $s(k)$ is recovered by simply dividing $y(k)$ with $\check{h}(k)$, dispensing with complex equalization. In the conventional system, $\check{h}(k)$ is estimated using pilots located at predetermined subcarriers with the following constraint: the channel responses in the time and frequency domains are related by

$$\check{\boldsymbol{h}} = \boldsymbol{F}_{N,L}\boldsymbol{h} \tag{2}$$

where $\boldsymbol{h} := (h[0], h[1], \ldots, h[L-1])^T$ and $\check{\boldsymbol{h}} := (\check{h}(0), \ldots, \check{h}(N-1))^T$. In practice, the number of subcarriers N, i.e., FFT block size, is designed to be significantly larger than the channel length [1]–[3], and hence, the range space of the channel in the frequency domain is restricted to a smaller L-dimensional space rather than the N-dimensional space.

In practical OFDM systems, a considerable fraction of subcarriers are reserved as guard subcarriers to eliminate interference from neighboring channels. Given the set of usable subcarriers

$$\mathcal{D} = \left\{0, 1, \ldots, \frac{N}{2} - \frac{N_G+1}{2}, \frac{N}{2} + \frac{N_G+1}{2}, \frac{N}{2} + \frac{N_G+1}{2}, \ldots, N-1\right\}$$

we may place pilots on a set of subcarriers $\mathcal{T} = \{i_1, i_2, \ldots, i_{N_p}\} \subset \mathcal{D}$.[1] For convenience, we assume the number of subcarriers N even and the number of guard subcarriers N_G odd. Without the constraint of (2), the associated channel can be estimated by $\hat{\check{h}}_P(i_l) = y(i_l)/s(i_l)$. To exploit the constraint in (2), we express the unconstrained channel estimate in a matrix form as

$$\begin{aligned}\hat{\check{\boldsymbol{h}}}_P &:= (y(i_1)/s(i_1), y(i_2)/s(i_2), \ldots, y(i_{N_p})/s(i_{N_p}))^T \\ &= \boldsymbol{F}_P\boldsymbol{h} + \boldsymbol{w}_P \end{aligned} \tag{3}$$

where $\boldsymbol{w}_P = (w(i_1)/s(i_1), \ldots, w(i_{N_p})/s(i_{N_p}))^T \in \mathcal{C}^{N_p}$ and $\boldsymbol{F}_P \in \mathcal{C}^{N_p \times L}$ denotes the DFT matrix of which entries are given as $[\boldsymbol{F}_P]_{l,k} = e^{-j\frac{2\pi}{N}i_l(k-1)}, \quad 1 \leq k \leq L, \quad 1 \leq l \leq N_p, \quad i_l \in \mathcal{T}$.

Since we are interested in estimating $\check{h}(k)$ only for usable subcarriers, the channel estimation problem can be stated as

1) *Problem:* given $\hat{\check{\boldsymbol{h}}}_P = \boldsymbol{F}_P\boldsymbol{h} + \boldsymbol{w}_P$, estimate $\check{\boldsymbol{h}}^G := \boldsymbol{F}_A\boldsymbol{h}$, where $[\boldsymbol{F}_A]_{l,k} = e^{-j\frac{2\pi i_l}{N}(k-1)}, 1 \leq k \leq L, 1 \leq l \leq N - N_G, \quad i_l \in \mathcal{D}$.

The ML and MMSE estimates of $\check{\boldsymbol{h}}^G$ can be obtained from those of $\boldsymbol{h}$ which is invariant to the presence of the guard subcarriers. Due to the invariance property of the ML estimator, the ML estimate for $\check{\boldsymbol{h}}^G$ is computed by $\hat{\check{\boldsymbol{h}}}^G_{\text{ML}} = \boldsymbol{F}_A\hat{\boldsymbol{h}}_{\text{ML}}$ where $\hat{\boldsymbol{h}}_{\text{ML}}$ is the ML estimate for $\boldsymbol{h}$ from (3). Similarly, the MMSE estimate for $\check{\boldsymbol{h}}^G$ can be obtained by a linear transformation of that for $\boldsymbol{h}$. The MMSE estimate is the conditional expectation of the desired parameter, and hence, the MMSE estimate is given as $\hat{\check{\boldsymbol{h}}}^G_{\text{MMSE}} = E[\boldsymbol{F}_A\boldsymbol{h}|\hat{\check{\boldsymbol{h}}}_P] = \boldsymbol{F}_A E[\boldsymbol{h}|\hat{\check{\boldsymbol{h}}}_P] = \boldsymbol{F}_A\hat{\boldsymbol{h}}_{\text{MMSE}}$, where $\hat{\boldsymbol{h}}_{\text{MMSE}} = E[\boldsymbol{h}|\hat{\check{\boldsymbol{h}}}_P]$. As a result, the estimation problem for $\check{\boldsymbol{h}}^G$ can be solved by that for $\boldsymbol{h}$.

First, consider $\boldsymbol{h}$ as a deterministic parameter. Then, $\hat{\check{\boldsymbol{h}}}_P$ can be modeled as a Gaussian random vector with $E[\hat{\check{\boldsymbol{h}}}_P] = \boldsymbol{F}_P\boldsymbol{h}$[2] and $\text{cov}[\hat{\check{\boldsymbol{h}}}_P] = N_0\boldsymbol{Q}_s^{-1}$, where $\boldsymbol{Q}_s := \text{diag}(|s(i_1)|^2, \ldots, |s(i_{N_p})|^2)$, then the LS and ML channel estimates $\hat{\boldsymbol{h}}_{\text{ML}}$ can be obtained by

$$\begin{aligned}\hat{\boldsymbol{h}}_{\text{LS}} &= \arg\min_{\boldsymbol{h}} ||\hat{\check{\boldsymbol{h}}}_P - \boldsymbol{F}_P\boldsymbol{h}||_2^2 \\ &= (\boldsymbol{F}_P^H\boldsymbol{F}_P)^{-1}\boldsymbol{F}_P^H\hat{\check{\boldsymbol{h}}}_P, \end{aligned} \tag{4}$$

$$\begin{aligned}\hat{\boldsymbol{h}}_{\text{ML}} &= \arg\min_{\boldsymbol{h}} (\hat{\check{\boldsymbol{h}}}_P - \boldsymbol{F}_P\boldsymbol{h})^H\boldsymbol{Q}_s(\hat{\check{\boldsymbol{h}}}_P - \boldsymbol{F}_P\boldsymbol{h}) \\ &= (\boldsymbol{F}_P^H\boldsymbol{Q}_s\boldsymbol{F}_P)^{-1}\boldsymbol{F}_P^H\boldsymbol{Q}_s\hat{\check{\boldsymbol{h}}}_P, \end{aligned} \tag{5}$$

where $\|\cdot\|_2$ denotes l_2-norm. Specially for quarternary phase shift keying (QPSK) signaling with $\boldsymbol{Q}_s = \sigma_s^2\boldsymbol{I}_N$, where $\sigma_s^2 = |s(k)|^2$, the ML estimator reduces to the LS estimator in Eq. (4), and also satisfies the Cramer–Rao lower bound (CRLB) [10]. If the channel is assumed random and the *a priori* distribution of the desired parameter $p(\boldsymbol{h})$ is available at the receiver and is Gaussian [e.g., $\boldsymbol{h} \sim \mathcal{C}N(\boldsymbol{m}_h, \boldsymbol{Q}_h)$], then the MMSE estimator can be obtained as

$$\begin{aligned}\hat{\boldsymbol{h}}_{\text{MMSE}} &= \arg\max_{\boldsymbol{h}} p(\boldsymbol{h}|\hat{\check{\boldsymbol{h}}}_P) \\ &= \boldsymbol{m}_h + (\boldsymbol{F}_P^H\boldsymbol{Q}_s\boldsymbol{F}_P + N_0\boldsymbol{Q}_h^{-1})^{-1}\boldsymbol{F}_P^H\boldsymbol{Q}_s(\hat{\check{\boldsymbol{h}}}_P - \boldsymbol{m}_h). \end{aligned} \tag{6}$$

Since our interest is to estimate $\check{h}(k)$ for usable subcarriers, the MSE of usable subcarriers in channel estimate should be defined

[1] It is also possible to write $\mathcal{D} = \{0, \pm 1, \pm 2, \ldots, \pm(\frac{N}{2} - \frac{N_G+1}{2})\}$.

[2] If $N_p \geq L$, then the DFT matrix $\boldsymbol{F}_P$ is a full rank matrix. It is possible to find a full rank $L \times L$ Van der Monde matrix in $\boldsymbol{F}_P$ [13]; and L column vectors of $\boldsymbol{F}_P$ containing independent column vectors of the Van der Monde matrix are also independent with each other, which proves that $\boldsymbol{F}_P$ is full rank. Subsequently, it is possible to find a unique least squares estimate for $\boldsymbol{h}$ based on (3).

accordingly as

$$\gamma^G := \sum_{k\in\mathcal{D}} E[|\check{h}(k) - \hat{\check{h}}(k)|^2]$$
$$= E[||\boldsymbol{F}_A(\boldsymbol{h} - \hat{\boldsymbol{h}})||_2^2] = E[(\boldsymbol{h} - \hat{\boldsymbol{h}})^H \boldsymbol{Q}_A (\boldsymbol{h} - \hat{\boldsymbol{h}})], \quad (7)$$

where $\boldsymbol{Q}_A := \boldsymbol{F}_A^H \boldsymbol{F}_A$. The MSE of each algorithm is then

$$\gamma_{\rm LS}^G = N_0 \,{\rm tr}\{\boldsymbol{F}_A(\boldsymbol{F}_P^H \boldsymbol{F}_P)^{-1}\boldsymbol{F}_A^H\} \quad (8)$$

$$\gamma_{\rm ML}^G = N_0 \,{\rm tr}\{\boldsymbol{F}_A(\boldsymbol{F}_P^H \boldsymbol{Q}_s \boldsymbol{F}_P)^{-1}\boldsymbol{F}_A^H\} \quad (9)$$

$$\gamma_{\rm MMSE}^G = N_0 \,{\rm tr}\{\boldsymbol{F}_A(\boldsymbol{F}_P^H \boldsymbol{Q}_s \boldsymbol{F}_P + N_0\boldsymbol{Q}_h^{-1})^{-1}\boldsymbol{F}_A^H\} \quad (10)$$

where $\gamma_{\rm LS}^G$, $\gamma_{\rm ML}^G$, and $\gamma_{\rm MMSE}^G$ represent the MSE for the LS, ML, and MMSE estimators, respectively. If there is no guard subcarrier (i.e., $\boldsymbol{Q}_A = N\boldsymbol{I}_L$), then the MSE for $\boldsymbol{h}$ $\gamma := NE[\|\boldsymbol{h} - \hat{\boldsymbol{h}}\|_2^2]$ is equal to γ^G, regardless of the type of the channel estimator. However, in general, it is not true that $\boldsymbol{F}_A^H\boldsymbol{F}_A \neq N\boldsymbol{I}_L$, and therefore, channel estimation errors for $\boldsymbol{h}$ may differ from those for $\check{\boldsymbol{h}}^G$. For each channel estimator, the MSEs for entire subcarriers are identified by $\gamma_{\rm LS} := NE[\|\boldsymbol{h} - \hat{\boldsymbol{h}}_{\rm LS}\|_2^2]$, $\gamma_{\rm ML} := NE[\|\boldsymbol{h} - \hat{\boldsymbol{h}}_{\rm ML}\|_2^2]$, and $\gamma_{\rm MMSE} := NE[\|\boldsymbol{h} - \hat{\boldsymbol{h}}_{\rm MMSE}\|_2^2]$, respectively.

For the block pilots and PSK signaling, i.e., $\boldsymbol{F}_A = \boldsymbol{F}_P$, the MSE for the ML estimator is obtained from Eq. (8) as $\gamma_{\rm ML}^G = N_0{\rm tr}\,\{\boldsymbol{F}_A(\boldsymbol{F}_A^H\boldsymbol{F}_A)^{-1}\boldsymbol{F}_A^H\} = N_0 L$, where ${\rm tr}\{AB\} = {\rm tr}\{BA\}$ is applied. This shows that the presence of guard subcarriers may increase only $\gamma_{\rm ML}$ and the numerical sensitivity of the matrix inversion of $\boldsymbol{Q}_A$, but not $\gamma_{\rm ML}^G$ of interest here. Similarly, the MSE for the MMSE channel estimate is given by $\gamma_{\rm MMSE}^G = N_0{\rm tr}\{\boldsymbol{F}_A^H\boldsymbol{F}_A(\boldsymbol{F}_A^H\boldsymbol{F}_A + N_0\boldsymbol{Q}_h^{-1})^{-1}\} \leq N_0 L$. In contrast to the LS and ML estimators, the MSE of the MMSE estimator may vary with the guard subcarriers due to the presence of $\boldsymbol{Q}_h^{-1}$ in $\gamma_{\rm MMSE}^G$.

III. Discussion on Pilot Design

If only a fraction of subcarriers are available for pilots, as is shown in (8)–(10), the MSE for the channel estimator is determined by placement of pilots and power loading through $\boldsymbol{F}_P$ and $\boldsymbol{Q}_s$, respectively. While optimal pilot placement to minimize the associated MSE for the MMSE estimator depends on statistics of the desired parameter, e.g., $\boldsymbol{Q}_h$, the comb pilots are optimal for the ML estimator in the sense of minimizing the MSE or maximizing the capacity [4], [6]. Due to the invariance of the ML and MMSE channel estimators under a linear transformation, optimality of the comb pilots still holds for the system with guard subcarriers. However, the number of guard subcarriers N_G limits the distance between adjacent pilots, say d, as $d \geq N_G$ and subsequently, the number of comb pilots N_p as $N_p \leq \lfloor \frac{N}{d} \rfloor$ where $\lfloor x \rfloor$ denotes the largest integer smaller than or equal to x. For example, in IEEE 802.11a and IEEE 802.16a standards, the number of equispaced pilots are upper bounded by 5 and 4, respectively, while they adopt $N_p = 4 < 5$ and $N_p = 8 > 4$, which implies that the comb pilots are impossible for IEEE 802.16a. Therefore, partially equispaced pilots $\mathcal{T} = \{-84, -60, -36, -12, 12, 36, 60, 84\}$ are considered instead [2].

When comb pilots are not allowed, in general, there is no closed-form expression relating pilot placement with the MSE, which makes pilot design complicated. In this section, though pilot design should take into account the combinations of the placement of pilots and power loading, we narrow our focus to the equal powered pilots for tractability, then pilot design can be restated by the optimization problem given by

$$\mathcal{T}_{\rm opt} = \arg\min_{\mathcal{T}} {\rm tr}\{(\boldsymbol{Q}_P(\mathcal{T}))^{-1}\} = \sum_{i=1}^{L} \frac{1}{\lambda_i(\boldsymbol{Q}_P(\mathcal{T}))} \quad (11)$$

where $\boldsymbol{Q}_P := \boldsymbol{F}_P^H\boldsymbol{F}_P$ and $\lambda_i(A)$ denotes the ith largest eigenvalue of the matrix A. Without constraints on the pilot subcarriers, the solution to the optimization problem in (11) is attained by comb pilots with uniform eigenvalues $\lambda_i(\boldsymbol{Q}_P(\mathcal{T})) = \lambda_{i+1}(\boldsymbol{Q}_P(\mathcal{T}))$ [6], otherwise, in general, $\mathcal{T}_{\rm opt}$ may be found by an exhaustive search over $N!/(N-N_p)!N_p!$ possible pilot allocations. Since exhaustive search requires tremendous numerical cost, we attempt to design pilots by examining asymptotic eigenvalues of $\boldsymbol{Q}_P$ in the presence of guard subcarriers, instead. First, it should be noted that $\boldsymbol{Q}_P$ is a Toeplitz matrix, since the entry of $\boldsymbol{Q}_P$ is a function of difference of indices, represented as

$$[\boldsymbol{Q}_P]_{l_1,l_2} = \sum_{k=1}^{n}[\boldsymbol{F}_P^H]_{l_1,k}[\boldsymbol{F}_P]_{k,l_2} = \sum_{k\in\mathcal{T}} e^{j\frac{2\pi}{N}kl_1}e^{-j\frac{2\pi}{N}kl_2}$$
$$= \sum_{k\in\mathcal{T}} e^{j\frac{2\pi}{N}(l_1-l_2)k}.$$

Also, define a pilot indicator function $R(k)$ as $R(k) = 1$ for $k \in \mathcal{T}$ and $R(k) = 0$ for else, then we can see that $\boldsymbol{Q}_P$ is an $L \times L$ Toeplitz matrix of which entries are obtained from a $2L-1$ length segment of N-point IDFT of $R(k)$, $r[n] = \sum_{k=0}^{N-1} R(k)e^{j\frac{2\pi}{N}nk}$ for $n = -L+1, -L+2, \ldots, L-2, L-1$. For example, given N_p partially d equispaced pilots symmetric about the origin

$$\mathcal{T} = \left\{ \pm\frac{d}{2}, \pm\frac{3d}{2}, \ldots, \pm\frac{d+(N_p-2)d}{2} \right\}$$

we can obtain entries of $\boldsymbol{Q}_P$ from N-point IDFT of $R(k)$ as

$$r[n] = \frac{\sin(\frac{\pi d}{N}N_p n)}{\sin(\frac{\pi d}{N}n)}. \quad (12)$$

Though the exact analytical expressions for eigenvalues of a general Toeplitz matrix are difficult to compute, the asymptotic equivalence of the Toeplitz and associated circulant matrices often helps understand and approximate its eigenstructure for some Toeplitz matrices such as the finite order Toeplitz matrix and the Toeplitz matrix constructed from absolutely summable sequences [16], [17]. In other words, a Toeplitz matrix of $r[n]$ decaying fast enough in n may be approximated by the associated circulant matrix. For the partially equispaced pilots, the energy of $r[n]$ in (12) attenuates rapidly with n, and thus, $\boldsymbol{Q}_P$ and its eigenvalues can be approximated with the associated circulant matrix and eigenvalues; since eigenvalues of a circulant matrix are the DFT of its first row, the eigenvalues of $\boldsymbol{Q}_P$ can be approx-

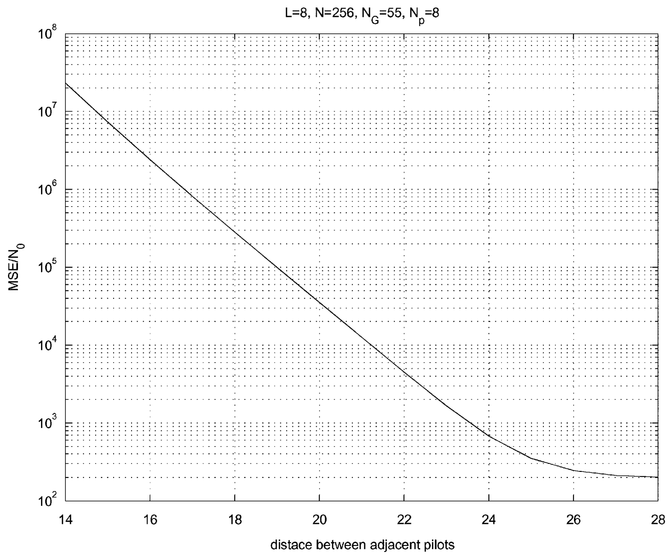

Fig. 1 MSE performance for partially equispaced pilots, $L = 8, N = 256, N_G = 55, N_p = 8$.

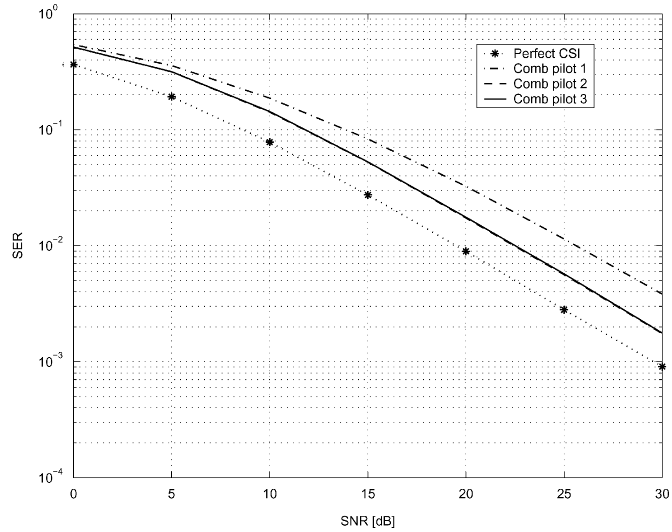

Fig. 2. SER performance for partially equispaced pilots, $Q = 4, L = 8, N = 256, N_G = 55, N_p = 8$.

imated by L-point DFT of the first row of the associated circulant matrix $\boldsymbol{c}_L := (r[0], r[1], \ldots, r[L/2], r[-L/2], r[-L/2+1], \ldots, r[-1])^T$, where L is even. In summary, the eigenvalues of $\boldsymbol{Q}_P$ can be approximated by the L-point DFT of the L data taken from the N-point IDFT of the pilot indicator function $R(k)$. As a result, considering that pilots with uniform eigenvalues produce the minimum MSE among all possible pilot placements [6], pilot design turns into determining a pilot indicator function $R(k)$ such that its N-point IDFT $r[n]$ has a narrower time duration or mainlobe to produce a more uniform L-point DFT of the truncated version of $r[n]$.[3] From (12), pilots with a larger distance d, will apparently have a narrower main lobe, and therefore, pilots with the largest d are expected to perform best. To show the validity of our claim, various pilot schemes were tested under scenarios consistent with OFDM systems of IEEE 802.16a standards, for which only partially equispaced pilots are possible. First, we tested the partially equispaced pilots with various distance with adjacent pilots, for instance,

$$\mathcal{T} = \left\{ \pm\frac{d}{2}, \pm\frac{3d}{2}, \ldots, \pm\frac{d + (N_p - 2)d}{2} \right\}$$

where $N_p = 8$ and $d \in [14, 28]$. Fig. 1 shows that the MSE is monotonically decreasing in the distance between pilots d, and this is consistent with the analytical results based on the asymptotic equivalence between the circulant and Toeplitz matrices. Second, the SER performance curve are obtained by averaging over 1000 random channels with $\boldsymbol{h} \sim \mathcal{C}N(0, \frac{1}{L}\boldsymbol{I}_L)$ and $L = 8$. Here, comb pilot 1 and comb pilot 2 denote the partially equispaced pilots with a distance $d = 24$, $\mathcal{T}_1 = \{-84, -60, -36, -12, 12, 36, 60, 84\}$ as in [2] and $d = 28$, $\mathcal{T}_2 = \{-98, -70, -42, -14, 14, 42, 70, 98\}$, respectively, and comb pilot 3 with $\mathcal{T}_3 = \{-100, -72, -44, -15, 15, 45, 72, 100\}$, which is designed to maximize the bandwidth covered with pilots by placing pilots on right and left ends of usable subcarriers. From the simulation result in Fig. 2, the comb pilot 2 and comb pilot 3 provide approximately 3-dB SNR gains for SER performance over comb pilot 1, respectively. From Eq. (9), the MSEs are given as $679N_0$, $202N_0$, and $197N_0$ for comb pilot 1, comb pilot 2, and comb pilot 3, respectively. Note that comb pilot 3 outperforms comb pilot 2 and this can be explained by the asymptotic eigenvalue distribution; the comb pilot 3 occupies larger bandwidth than the comb pilot 2 and produces a narrower pulse in the time domain and subsequently more uniform eigenvalues, which in turn leads to a smaller MSE.

IV. Channel Estimation with FIR Approximation

For systems with guard subcarriers, the matrix inversion and associated matrix multiplication in (5) and (6) requires additional hardware, and the numerical complexity of the ML and MMSE channel estimators increase rapidly with the channel length. By assuming the maximum channel length, say $L_{\max}$, and performing the matrix inversion in advance, we can implement the ML channel estimator at $2N \log N + L^2$ complex multiplications. In this case, as the maximum channel length $L_{\max}$ tends to increase with the number of subcarriers N, i.e., $L_{\max} = N/32, N/16, N/8, N/4$ [1], [2], the numerical complexity of the ML channel estimator and memory required to save the inverse matrix in (5) become dominated by $O(N^2)$. As a result, the ML and MMSE channel estimator is not practical for communication systems using a large number of subcarriers, e.g., $N = 2048$ and $N = 8192$ for IEEE 802.16a and for the digital video broadcasting–handheld (DVB-

[3] It may be interpreted by the Gershgorin circle theorem [13], which says the eigenvalues of matrix $\boldsymbol{Q}_P$ all lie in the union of the Gershgorin disks of $\boldsymbol{Q}_P$: $\lambda(\boldsymbol{Q}_P) \subset \cup_{i=1}^m R_i(\boldsymbol{Q}_p)$, where $R_i(\boldsymbol{Q}_p) = \{x \in \mathcal{C} : |x - r[0]| = |x - 1| \leq \sum_{j=1, j\neq i}^L |r[i-j]|\}$. Therefore, with $|r[n]|$ decaying fast enough in $|n|$, i.e., $\sum_{j=1, j\neq i}^L |r[i-j]|$ is very small, all eigenvalues $\boldsymbol{Q}_p$ are very close to 1 and uniform eigenvalues.

H) standards, respectively [1], [2]. In this section, we propose a suboptimal but efficient channel estimator without need for matrix inversion and associated complex multiplication by introducing an extended channel and its FIR approximation. For clarity, we consider block pilots, while extension to the partially equispaced pilots is straightforward. The presence of guard subcarriers can be dealt with by introducing the compound system of $\check{h}_e(k) := A(k)\check{h}(k)$, where $A(k) = 1$ for all usable subcarriers and $A(k) = 0$ for else. It is noted that an estimate of $\check{h}_e(k)$ is sufficient for equalization concerning usable subcarriers, since $\check{h}_e(k)$ is equal to $\check{h}(k)$ for usable subcarriers. Equivalently we can define the IDFT of $\check{h}_e(k)$ as an extended channel $h_e[n] := a[n] \odot_N h[n]$ in the time domain, where $\odot_N$ denotes an N-point circular convolution and $a[n]$ is the N-point IDFT of $A(k)$. In contrast to $h[n]$, which is the FIR of length L, $h_e[n]$ stretches over N samples in the time domain, since $a[n]$ is a length N sequence with

$$|a[n]| = \frac{|\sin(\frac{\pi}{N} N_G n)|}{|\sin(\frac{\pi}{N} n)|}.$$

Therefore, the range space of $\check{\boldsymbol{h}}_e := (\check{h}_e[0], \check{h}_e[1], \ldots, \check{h}_e[N-1])^T$ is N-dimensional, which makes noise reduction impossible for general estimation of $\boldsymbol{h}_e := (h_e[0], h_e[1], \ldots, h_e[N-1])^T$. However, we know that the energy of $a[n]$ is concentrated within a relatively short time duration about the origin, which enables approximation of $h_e[n]$ by a channel with a shorter length, termed an FIR approximation to $h_e[n]$ and improving channel estimates through denoising.

A. FIR Approximation

In the presence of guard subcarriers, we may rewrite (3) in terms of $\boldsymbol{h}_e$ by

$$\begin{aligned} \tilde{\check{\boldsymbol{h}}}_P &:= \boldsymbol{G}\check{\boldsymbol{h}}_P = \boldsymbol{G}\boldsymbol{F}_{N,L}\boldsymbol{h} + \boldsymbol{G}\boldsymbol{w}_P \\ &= \boldsymbol{F}_{N,N}\boldsymbol{h}_e + \boldsymbol{G}\boldsymbol{w}_P \end{aligned} \quad (13)$$

where $\boldsymbol{G} \in \mathcal{C}^{N\times N}$ with $[\boldsymbol{G}]_{i,j} = 1$ for $i = j \in \mathcal{D}$ and $[\boldsymbol{G}]_{i,j} = 0$, elsewhere. For QPSK signaling, the LS estimate for $\boldsymbol{h}_e$ is obtained by $\hat{\boldsymbol{h}}_{e,LS} = \frac{1}{N}\boldsymbol{F}_{N,N}^H \tilde{\check{\boldsymbol{h}}}_P$ and results in the MSE, $\gamma_{e,LS} = \frac{N-N_G}{NN_0}$. From (13), it is seen that the LS estimator for $\boldsymbol{h}_e$ can be implemented with an N-point inverse FFT (IFFT) without matrix inversion, while the lack of denoising causes significant estimation errors compared to the LS estimator for $\boldsymbol{h}$. However, noting that the energy of $a[n]$ decays as $1/n$, we may use a $2L_c + 1$ FIR approximation to $a[n]$ as $\tilde{a}[n] = a[n]$ for $|n| \leq L_c$ and $\tilde{a}[n] = 0$ for elsewhere, where L_c is a truncation threshold. Then, taking the L_c right cyclic shift on $\boldsymbol{h}_e$, we can write $\boldsymbol{h}_e$ in terms of the assumed length $2L_c + L$ FIR channel $\bar{\boldsymbol{h}}_e := (h_e[-L_c], \ldots, h_e[L + L_c - 1])^T$ and the associated approximation error $\tilde{\boldsymbol{h}}_e := (h_e[L + 2L_c], \ldots, h_e[N - L_c - 1])^T$ as $\boldsymbol{h}_e = (\bar{\boldsymbol{h}}_e^T \tilde{\boldsymbol{h}}_e^T)^T$. Then, (3) can be written as

$$\boldsymbol{y}_e := \boldsymbol{C}\tilde{\check{\boldsymbol{h}}}_P = \boldsymbol{F}_C\bar{\boldsymbol{h}}_e + \boldsymbol{F}_C^{\perp}\tilde{\boldsymbol{h}}_e + \boldsymbol{C}\boldsymbol{G}\boldsymbol{w}_P \quad (14)$$

where $\boldsymbol{C} \in \mathcal{C}^{N\times N}$ represents the right cyclic shift by L_c and $\boldsymbol{F}_C \in \mathcal{C}^{N\times(L+2L_c)}$ is the DFT matrix with $[\boldsymbol{F}_C]_{l,k} = e^{-j\frac{2\pi}{N}(l-1)(k-Lc-1)}, 1 \leq l \leq N, 1 \leq k \leq L + 2L_c$, and $[\boldsymbol{F}_C^{\perp}]_{l,k-L-2L_c} = e^{-j\frac{2\pi}{N}(l-1)(k-Lc-1)}, 1 \leq l \leq N, L + 2L_c + 1 \leq k \leq N$. Since $\boldsymbol{C}\boldsymbol{F}_C^{\perp}\tilde{\boldsymbol{h}}_e \perp \mathcal{R}(\boldsymbol{F}_C)$ in (14), the LS estimate for $\bar{\boldsymbol{h}}_e$ and the associated MSE are given by

$$\bar{\boldsymbol{h}}_{e,LS} = \frac{1}{N}\boldsymbol{F}_C^H\boldsymbol{y}_e \quad (15)$$

$$\bar{\gamma}_{\mathrm{LS}}(L_c) := E[||\bar{\boldsymbol{h}}_e - \bar{\boldsymbol{h}}_{e,LS}||_2^2] = \frac{L + 2L_c}{N - N_G}N_0. \quad (16)$$

Also, we can select L_c to minimize the MSE, by analyzing the approximation error caused by the FIR approximation. Given L_c, we can calculate the mean-squared approximation error $\tilde{\gamma}_{\mathrm{LS}}(L_c)$ by

$$\begin{aligned} \tilde{\gamma}_{\mathrm{LS}}(L_c) &= \sum_{n=L+L_c}^{N-L_c} E[|h_e[n]|^2] \\ &= \sum_{n=L+L_c}^{N-L_c} E\left[\left|\sum_{k=0}^{L-1} h[k]a[(n-k)_N]\right|^2\right]. \end{aligned} \quad (17)$$

where $()_N$ denotes the modulo N operation. Then, the MSE $\gamma_{\mathrm{FIR}}(L_c)$ for the LS estimator can be expressed in terms of $\bar{\gamma}_{\mathrm{LS}}(L_c)$ and $\tilde{\gamma}_{\mathrm{LS}}(L_c)$ as $\gamma_{\mathrm{FIR}}(L_c) = \bar{\gamma}_{\mathrm{LS}}(L_c) + \tilde{\gamma}_{\mathrm{LS}}(L_c)$. Since $\bar{\gamma}_{\mathrm{LS}}(L_c)$ from the additive noise increases linearly with L_c, and $\tilde{\gamma}_{\mathrm{LS}}(L_c)$ accounting for the approximation error is inversely related with L_c, we can find an optimal L_c minimizing $\gamma_{\mathrm{FIR}}(L_c)$ by an exhaustive search given by

$$\hat{L}_c = \arg \min_{L_c \in \{0,1,\ldots,\lceil (N-L)/2 \rceil\}} \frac{\gamma_{\mathrm{FIR}}(L_c)}{N_0}$$

where $\lceil x \rceil$ represents a smallest integer larger than x.

B. Implementations

In this section, we discuss two different implementations of the channel estimator based on FIR approximation, FFT-based implementation, and LPF-based implementation. From (15), the final channel estimate in the frequency domain is computed by

$$\check{\boldsymbol{h}}_{e,LS} = \frac{1}{N}\boldsymbol{F}_C\boldsymbol{F}_C^H\boldsymbol{y}_e \quad (18)$$

which can be implemented simply by FFT and IFFT as the ML estimator without guard subcarriers. However, the FFT-based algorithm has a couple of problems for its practical use. First, numerical complexity of the FFT may become significant for OFDM systems with a large number of subcarriers used. Second, FFT-based algorithms needs to run FFT twice to get the final channel estimate, and this may cause the bottleneck effect before an FFT block that is frequently accessed for both uplink and downlink communications. Third, FFT is basically a batch algorithm, which processes all data from N subcarriers and also produces N output at one time, and thus, this requires a relatively large memory size and time delay. Especially for OFDMA systems, where only a fraction of subcarriers, say

$N_{\rm sub}$, are allotted to a subscriber, i.e., $N_{\rm sub} \le N$, the numerical complexity and time delay of the FFT-based algorithm remain high.

Equivalently, noting that $\boldsymbol{F}_C \boldsymbol{F}_C^H$ is a Toeplitz matrix, an ideal frequency domain LPF that rejects data at time indices $n \notin \{-L_c, -L_c+1, \ldots, L+L_c-1\}$ in the time domain, can be used for (18), but with the higher numerical complexity of $O(N_{\rm sub}N)$. Alternatively, at the cost of moderate performance loss, we can use an $N_{\rm tap}$ tap LPF with the numerical complexity $O(N_{\rm sub}N_{\rm tap})$, designed to approximate an ideal LPF with the low and high cutoff time indices $t_{\rm lc} = -L_c - 1$ and $t_{\rm hc} = L + L_c$, respectively. In practice, we choose $t_{\rm lc} < -L_c - 1$ and $t_{\rm hc} > L + L_c$ in order not to introduce channel distortions from the unflat passband. The merits of the LPF-based algorithm are summarized here.

1) Differently from the FFT-based algorithm, the LPF-based algorithm can select subcarriers of interest and produce channel estimates associated with those without a large time delay.
2) In contrast to the FFT that implements the DFT consisting of N complex additions and multiplications, the LPF uses $N_{\rm tap}$ data to obtain a channel estimate, which implies a narrower range of intermediate data in the channel estimator. Therefore, data bitwidth required to achieve a desired signal-to-quantization-noise-ratio (SQNR) for the LPF-based algorithm is far less than that for the FFT-based algorithm; for e.g., given uniformly distributed input, the 2048-point FFT requires 13 bits to attain an SQNR of 40 dB, compared with 7 bits for an LPF of $N_{\rm tap} = 40$ [14].
3) Hardware implementation of an $N_{\rm tap}$ tap LPF is relatively simpler than FFT block; FFT requires N data buffers to save the input and output from each FFT stage and a complex control logic.

In the following, we tested the proposed channel estimation algorithm, and compared its performance with other algorithms in terms of the SER.

C. Example

Consider OFDMA systems with $N = 2048, N_G = 345$, and $N_{\rm sub} \le 1703$ and QPSK pilots as in the IEEE 802.16a standard [2]. Pilots are located at even usable subcarriers, and nulls at odd subcarriers, which is consistent of preambles in the IEEE 802.16a standard [2]. The SER curves were obtained by averaging over 1000 random channels with $\boldsymbol{h} \sim \mathcal{C}N(0, \frac{1}{L}\boldsymbol{I}_L)$ and $L = N/16 = 128$. The channel estimator parameter L_c is fixed at 50 for the FFT-based channel estimator. An LPF of $N_{\rm tap} = 40$ is designed to have cut-off time indices $t_{\rm hc} = -t_{\rm lc} = 200$ and the real coefficients. In this case, the number of complex multiplications required for the LPF-based algorithm is $N_{\rm sub}(N_{\rm tap}/4)$, where a factor of 4 accounts for the use of the real coefficient, and the fact that at least half of subcarriers have 0 in the preamble because of the way it was generated. According to our simulations, the performance of the LPF-based algorithm was saturated approximately at 7 bits, but the FFT-based algorithm and ML algorithm did at 16 bits and at 17 bits,

TABLE I
NUMERICAL COMPLEXITY ($N = 2048, N_{\rm tap} = 40$˜$L = N/16$)

	LPF-based algorithm	FFT-based algorithm	ML algorithm
Bit width	7	16	17
# of complex mults.	$N_{sub}\frac{N_{tap}}{4} \le 17030$	$2N\log_2 N = 45056$	$2N\log_2 N + L^2 = 61440$
# of 16 bit complex mults.	≤ 3264	45056	69360

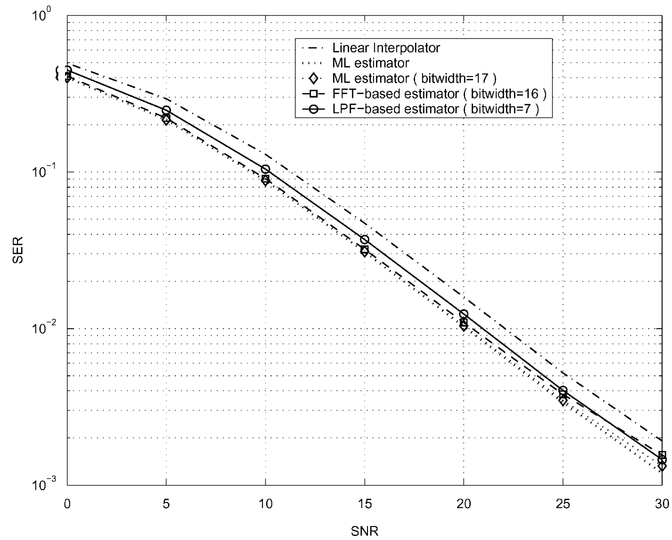

Fig. 3 SER performance of the channel estimators based on the FIR approximation, $Q = 4, L = 128, N = 2048, N_G = 345$.

respectively. In Table I, the algorithms are compared in terms of 16-bit complex multiplications required.[4]

Note that the numerical complexity of the LPF-based algorithm is linear in N, while those of the FFT-based algorithm and ML algorithm are $O(N \log N)$ and $O(N^2)$, respectively. Consider $L = N/4 = 512$, for, redundant "for" e.g., then the hardware complexity of the ML algorithm is tremendous and thus impractical, as it requires 307 200 complex multiplications and the storage of the size of $L^2 = 262144$ to save the associated inverse matrix. The SER performance for the various channel estimators are compared in Fig. 3. The ML estimator outperforms the linear interpolator by 2 dB in terms of symbol error rate (SER), while the performance of the channel estimator with an FIR approximation lies between them. At low SNRs, the FIR approximation provides a maximum SNR gain of 2 dB over the linear interpolator, while the performance difference becomes tapered as the SNR increases; the error from the FIR approximation $\tilde{\gamma}_{\rm LS}(L_c)$ begins to dominate the channel estimation error $\gamma_{\rm FIR}(L_c)$. By the proper selection of L_c based on the SNR, instead of using the fixed L_c, we can see that the LPF-based channel estimator exhibits the SNR gain of 1.2 dB over the linear interpolator at the relatively low numerical complexity.

V. CONCLUSION

We investigated LS, ML, and MMSE channel estimators for OFDM systems with guard subcarriers. The effect of guard

[4]The numerical complexity of B bit multiplications is given as $O(B^2)$, and thus, the complexity of 6-bit multiplications should be scaled down by a factor of $16^2/6^2 = 7.1$ compared with that for 16-bit multiplications.

subcarriers was examined by the asymptotic equivalence between the Toeplitz and associated circulant matrices, and it was also shown that given the number of pilots, pilots with the largest possible distance between adjacent subcarriers provide the best channel estimate among partially equispaced pilots. In addition, we developed a suboptimal low complexity algorithm by introducing an extended channel and its FIR approximation, followed by two different implementations based on FFT and LPF.

REFERENCES

[1] European Standards for Broadcasting, "Digital broadcasting system television, sound, and data services; Framing structure, channel coding, and modulation digital terrestrial television," Eur. Telecommun. Stand. Inst., Sophia-Antipolis, Valbonne, France, 2004, ETS 300 744.

[2] *Wireless LAN and MAN Medium Access Control (MAC) and Physical Layer (PHY) Specifications*, IEEE 802.16a, 2002.

[3] *Wireless LAN Medium Access Control (MAC) and Physical Layer (PHY) Specifications*, IEEE Standard 802.11a, 1999.

[4] S. Adireddy, L. Tong, and H. Viswanathan, "Optimal embedding of known symbols for OFDM," in *Proc. ICASSP'01*, May 2001, vol. 4, pp. 2393–2396.

[5] M. Dong, L. Tong, and B. M. Sadler, "Optimal pilot placement for channel tracking in OFDM," in *Proc. MILCOM'02*, Washington, DC, Oct. 2002, vol. 1, pp. 602–606.

[6] R. Negi and J. Cioffi, "Pilot tone selection for channel estimation in a mobile OFDM system," *IEEE Trans. Consum. Electron.*, vol. 44, no. 3, pp. 1122–1128, Aug. 1998.

[7] I. Barhumi, G. Leus, and M. Moonen, "Optimal training design for MIMO OFDM systems in mobild wireless channels," *IEEE Trans. Signal Process.*, vol. 51, no. 6, pp. 1615–1624, Jun. 2003.

[8] J. Rinne and M. Renfors, "Pilot spacing in orthogonal frequency division multiplexing systems on practical channels," *IEEE Trans. Consum. Electron.*, vol. 42, no. 4, pp. 959–962, Nov. 1996.

[9] O. Edfors and M. Sandell et al., "OFDM channel estimation by singular value decomposition," *IEEE Trans. Commun.*, vol. 46, no. 7, pp. 931–939, Jul. 1998.

[10] M. Morelli and U. Mengali, "A comparison of pilot-aided channel estimation methods for OFDM systems," *IEEE Trans. Signal Process.*, vol. 49, no. 12, pp. 3065–3073, Dec. 2001.

[11] Y. Li, L. J. Cimini, Jr., and N. R. Sollenberger, "Robust channel estimation for OFDM systems with rapid dispersive fading channels," *IEEE Trans. Commun.*, vol. 46, no. 7, pp. 902–915, Jul. 1998.

[12] Y. Li, "Pilot-symbol-aided channel estimation for OFDM in wireless systems," *IEEE Trans. Vehicular Tech.*, vol. 49, no. 4, pp. 1207–1215, Jul. 2000.

[13] T. K. Moon and W. C. Stirling, *Mathematical Methods and Algorithms for Signal Processing*. Englewood Cliffs, NJ: Prentice Hall, 2000.

[14] A. V. Oppenheim and R. W. Schafer, *Digital Signal Processing*. Englewood Cliffs, NJ: Prentice-Hall, 1998.

[15] B. Hassibi and B. Hochwald, "How much training is needed in multiple-antenna wireless links," *IEEE Trans. Inf. Theory*, vol. 49, no. 4, pp. 951–963, Apr. 2003.

[16] R. M. Gray, "On the asymptotic eigenvalue distribution of Toeplitz Matrices," *IEEE Trans. Inf. Theory*, vol. 18, no. 6, pp. 725–730, Nov. 1972.

[17] U. Grenander and G. Szegö, *Toeplitz Forms and Theri Applications*. Berkeley, CA: Univ. California Press, 1958.